RESEARCH ARTICLE

DOI: 10.54926/jnamt.2026.2641

J Nav Architect Mar Technol 2026;228:32-42

Effect of Hull Form Variations on Slamming and Dynamic Response in a Naval Vessel

Marcelo de Oliveira Predes

Brazilian Navy, Rio de Janeiro, Brazil

To cite this article: M. O. Predes. Effect of hull form variations on slamming and dynamic response in a naval vessel. *J Nav Architect Mar Technol*. 2026;228:32-42.

Received: 13.01.2026 - **Revision Requested:** 14.02.2026 - **Last Revision Received:** 23.02.2026 - **Accepted:** 02.03.2026 - **Publication Date:** 17.03.2026

Abstract

This study evaluates the influence of specific hull-form parameters on slamming behavior. The hull of a military frigate was adopted as the baseline geometry, and systematic variations were generated by modifying one form parameter at a time. Ship motions were evaluated using a strip-theory-based seakeeping program, from which radiation damping and hydrostatic restoring coefficients were obtained, together with relative displacements and velocities at the critical hull location. Slamming occurrence frequency was then estimated by combining the motion responses with long-term wave statistics, allowing a probabilistic assessment under realistic sea conditions. The results indicate that variations in hull geometry, particularly near the waterplane area, significantly influence the probability of slamming. The main contribution of this work lies in the direct and isolated evaluation of hull-form parameters and their quantitative relationship with slamming behavior and global dynamic response, providing practical insights for hull-form optimization during the preliminary design stage.

Keywords: Slamming probability, Hull form variation, Ship seakeeping, Dynamic response analysis

1. Introduction

Within seakeeping dynamics, slamming is typically defined as the violent impact of a ship's hull against the water surface. These events can cause damage to onboard equipment and compromise the vessel's structural integrity. Their occurrence and severity are closely linked to both environmental conditions and specific hull design features, potentially limiting a ship's operational effectiveness. Consequently, reducing the likelihood of slamming and its associated impact forces has become a key objective in naval architecture, especially for vessels operating at high speeds or in rough seas. To optimize hull form regarding seakeeping, it is essential to recognize that a ship's dynamic behavior is largely governed by global variations in geometry [1]. Thus, refining hull parameters during the early design stages is crucial to improving overall performance. A practical approach involves characterizing the hull using a set of geometric parameters that allow for systematic performance evaluation.

Several studies have adopted this strategy. Bales [2] applied regression analysis to correlate destroyer-type hull responses with specific form parameters. Lloyd [3] analyzed the influence of hull size and shape on the vertical motions of a frigate, assessing absolute vertical acceleration and relative bow displacement-linked respectively to crew comfort and slamming occurrence. The study concluded that larger hulls (with unchanged form) exhibited attenuated vertical motions. It also found that a lower draft-to-length ratio generally reduced motions but increased the likelihood of keel emergence. Additionally, increasing the forward waterplane area coefficient (C_{WP}) was shown to reduce both absolute

Address for Correspondence: Marcelo de Oliveira Predes, Brazilian Navy, Rio de Janeiro, Brazil
E-mail: marcelo.o.predes@gmail.com
ORCID ID: orcid.org/0009-0001-2189-4088

Copyright© 2026 The Author(s). Published by Galenos Publishing House on behalf of UCTEA Turkish Chamber of Naval Architects and Marine Engineers.
Licensed under a Creative Commons Attribution-NonCommercial-NoDerivatives 4.0 (CC BY-NC-ND) International License

and relative vertical motions and decrease keel emergence probability. In a more recent contribution, [4] investigated seakeeping improvements in a catamaran-type vessel using parametric transformations via the Lackenby method. The study varied block coefficient (C_B) and longitudinal center of buoyancy (*LCB*) by ±10% relative to a baseline model. Analyses were conducted under both regular and irregular wave conditions, incorporating regional sea characteristics. All generated hulls were verified for stability and resistance. Results indicated that variations in *LCB* and C_{WP} significantly influenced seakeeping, while changes in C_B had relatively minor effects. Hakim et al. [5] performed a comparative analysis of slamming probability between U- and V-shaped hull sections using strip theory. Their findings showed that U-shaped hulls had a 20-35% higher likelihood of slamming, emphasizing the role of hull section geometry in impact vulnerability.

More recently, computational fluid dynamics (CFD) methods have been employed to provide deeper insights into slamming and seakeeping behavior. Liao et al. [6] used a Reynolds-averaged Navier–Stokes-based CFD solver with overset grids to analyze trimaran seakeeping and slamming in oblique waves, highlighting distinct behaviors from monohulls and revealing severe bow slamming and green water events under varying speeds and headings. Kapsenberg [1], in earlier work on hull optimization, proposed a methodology combining polynomial functions and Lewis transformations to generate new hull forms. While his method yielded notable performance improvements, the resulting geometries were deemed unrealistic for practical application.

Building upon these foundations, the present study investigates how variations in selected hull form parameters affect a ship's dynamic behavior, with particular emphasis on slamming prediction. The proposed methodology involves independent variation of each parameter, enabling isolated assessment of its influence on ship motions and slamming probability. The analysis incorporates seakeeping simulations based on linear potential theory, including excitation forces, damping coefficients, and relative motions and velocities at a critical point near the bow keel, where slamming is most likely to occur.

2. Parametric Hull Form Variations

This study uses the hull of the Dutch frigate Friesland as the reference geometry for analysis. Figure 1 presents the body plan of the reference geometry, reconstructed from the original offsets data, which serves as the basis for the implemented Bézier and Lewis sectional modifications. The main characteristics of the baseline hull are summarized in Table 1.

Table 1. Main characteristics.

L_{PP}	112.4 m
B	11.74 m
T	4.01 m
C_B	0.562
Pitch radius of gyration	0.233 L_{PP}
Displacement	3046 tons

Due to their relatively smaller size compared to large commercial vessels and their high-speed operational profile, frigates are particularly susceptible to slamming events. Such impacts can damage not only the ship's structure but also critical onboard systems such as sensors, weapons, and ammunition. Hull geometry and seakeeping data for this vessel type are available in [7], which provided the foundation for model generation.

To investigate the influence of specific geometric features on ship response, four hull form parameters were selected for variation:

1. Longitudinal Center of Buoyancy (LCB/L_{PP}),
2. Block Coefficient (C_B),

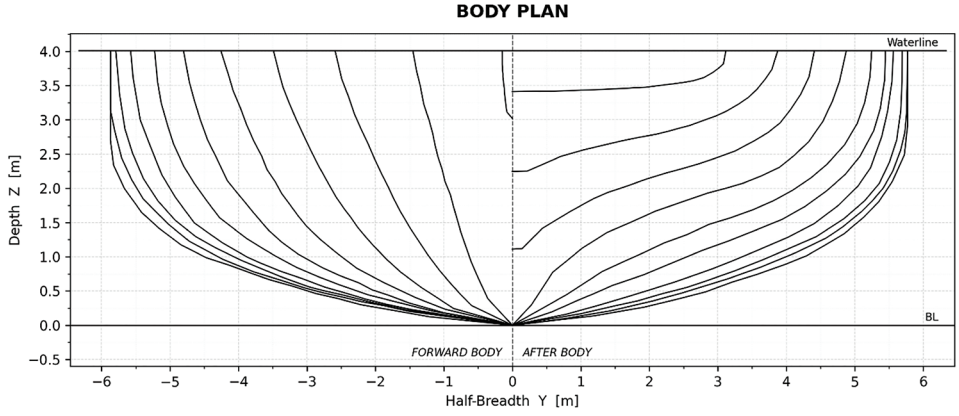

Figure 1. Body plan of the frigate Friesland.

3. Longitudinal Center of Flotation (LCF/L_{PP}),

4. Waterplane Area Coefficient (C_{WP}).

A custom algorithm was developed to generate a large number of hull geometries derived from the baseline model. A filtering process was then applied to retain only those variants in which a single parameter deviated meaningfully from the original configuration, while the remaining three parameters remained close to their baseline values. This ensures that each selected variation isolates the influence of one geometric factor, enabling valid comparative analysis. From this filtered set, the most extreme values observed for each parameter—maximum and minimum—were chosen to define the eight final configurations used in the study:

- *LCB* (+): center of buoyancy shifted forward,
- *LCB* (-): center of buoyancy shifted aft,
- C_B (+): higher block coefficient (fuller hull),
- C_B (-): lower block coefficient (finer hull),
- *LCF* (+): center of flotation shifted forward,
- *LCF* (-): center of flotation shifted aft,
- C_{WP} (+): higher waterplane area coefficient,
- C_{WP} (-): lower waterplane area coefficient.

The complete methodology used to generate, filter, and select the hull variants is detailed in previous work [8], which outlines the geometric framework adopted. A later publication [9] complements this discussion by offering further analysis and interpretations of the parametric variation approach. Based on that process, eight extreme configurations were identified, each designed to isolate the effect of a single hull form parameter while keeping the remaining parameters approximately constant. Notably, more pronounced variations were achieved for the LCF/L_{PP} and C_{WP} parameters, whereas the LCB/L_{PP} and C_B variations were more constrained due to the geometric interdependencies. In order to verify the basic feasibility of the selected variants, all eight hulls were subjected to preliminary stability analyses. Intact stability was assessed according to the criteria defined by the International Maritime Organization (IMO) in Resolution A749(18) (IMO, 1993), and all configurations were found to be compliant. The final values associated with each extreme case are summarized in Table 2.

In addition to the geometric constraints previously described, the normal draft, maximum beam, length between perpendiculars, and the longitudinal profile were kept constant for all hull variants. Furthermore, the sectional beam distribution along the hull was interpolated using a second-degree polynomial function in order to avoid abrupt contour variations at the waterplane. These measures ensured geometric smoothness and consistency across all configurations. Although the selected cases represent extreme values within the investigated parameter ranges, the resulting hull forms remain within the family of conventional displacement ships, preserving sectional characteristics compatible with the assumptions underlying linear strip theory.

3. Mathematical Formulation

3.1. Governing Theory and Hydrodynamic Model

The hydrodynamic modeling adopted in this study is based on linear potential flow theory within the strip theory framework. The fluid domain is assumed to be incompressible, inviscid and irrotational, which permits the use of a velocity potential ϕ that satisfies the Laplace equation (Equation 1):

$$\nabla^2 \phi = 0 \tag{1}$$

This potential must also satisfy boundary conditions at the free surface, hull surface, sea bottom (if applicable), and at infinity. The ship is modeled as a rigid body advancing at constant forward speed in calm water, disturbed by regular or irregular waves. For ships with longitudinal symmetry and slender hull forms, the hydrodynamic forces in surge (longitudinal translation) are significantly smaller than those in heave and pitch and can be neglected without compromising accuracy. Therefore, the system of equations is simplified by considering only vertical (heave) and angular (pitch) motions in the vertical plane. Figure 2 illustrates the coordinate system adopted in this study, with the origin located at the center of gravity (CG). The x-axis is aligned with the ship's longitudinal direction, the z-axis is positive upwards, and the y-axis completes the right-handed coordinate system.

The equations of motion in the frequency domain for heave and pitch are given by Equation (2):

$$\left[-\omega^2(M + A(\omega)) + i\omega B(\omega) + C\right] \eta(\omega) = F(\omega) \tag{2}$$

Table 2. Extreme values.

Parameter	Base	*LCB* (-)	*LCB* (+)	C_B (-)	C_B (+)	*LCF* (-)	*LCF* (+)	C_{WP} (-)	C_{WP} (+)
LCB/L_{PP}	0.489	0.447	0.510	0.358	0.590	0.435	0.515	0.777	0.867
C_B	0.562	0.563	0.561	0.490	0.489	0.793	0.793	0.463	0.460
LCF/L_{PP}	0.461	0.462	0.461	0.462	0.462	0.489	0.491	0.492	0.492
C_{WP}	0.794	0.796	0.792	0.796	0.796	0.560	0.559	0.561	0.561

LCB: Longitudinal center of buoyancy, *LCF*: Longitudinal center of flotation

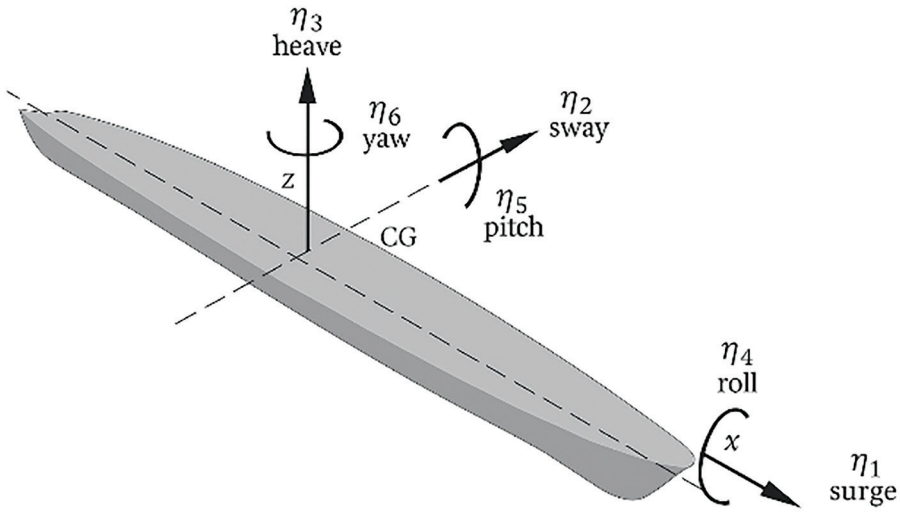

Figure 2. Coordinate system and six degrees of freedom used in the hydrodynamic analysis (adapted from [8]).

Where ω is the encounter frequency, M is the mass matrix, $A(\omega)$ is the added mass, $B(\omega)$ is the radiation damping, C is the hydrostatic restoring stiffness, $\eta(\omega)$ is the motion response vector (heave and pitch), and $F(\omega)$ is the wave excitation force vector. For the parametric hull variants analyzed in this study, the rigid-body mass matrix M was updated to account for the corresponding displacement variations. However, the pitch radius of gyration about the transverse axis was assumed constant and equal to that of the baseline hull. This simplifying assumption was adopted due to the complexity associated with reliably estimating structural mass redistribution for each geometric modification. Therefore, variations in pitch response are primarily attributed to hydrodynamic and hydrostatic changes rather than modifications in mass distribution.

To obtain the hydrodynamic coefficients and wave loads, strip theory is applied as formulated by [10]. The hull is divided into transverse sections, and the two-dimensional potential problem is solved at each section. The global response is then determined by integrating along the ship's length. This approach provides a practical compromise between computational efficiency and accuracy, especially for seakeeping evaluations of slender hulls in moderate sea states. The simulations in this work were conducted using the Seaway Octopus software, which implements this methodology.

3.2. Ship Response in Waves

The ship's dynamic behavior under wave excitation was evaluated through simulations in both regular and irregular seas, using linear frequency-domain potential theory. In the regular wave approach, the vessel is subjected to monochromatic waves across a range of encounter frequencies to determine its fundamental response characteristics. This results in the response amplitude operators (RAOs), which quantify the motion response as a function of frequency and serve as the foundation for spectral analysis in irregular seas. To compute the motion response $\eta(\omega)$ at each frequency, the linear equations of motion described in Section 3.1 are solved in the frequency domain (Equation 3):

$$\eta(\omega) = -\left[-\omega^2(M + A(\omega)) + i\omega B(\omega) + C\right]^{-1} * F(\omega) \quad (3)$$

The RAO for each motion component is given by Equation (4):

$$\mathrm{RAO}_{\eta}(\omega) = \left|\frac{|\eta(\omega)|}{|\zeta_a|}\right| \quad (4)$$

Where ζ_a is the wave amplitude and $\eta(\omega)$ is the complex motion amplitude. In this study, the analysis focused on heave (η_3) and pitch (η_5), while surge, roll, and yaw were neglected due to the longitudinal symmetry of the hull and the head-sea wave condition. Local kinematic responses were also evaluated at a specific analysis point P, located 10% of the ship length from the forward perpendicular, at the keel level. This location lies within the forward impact region commonly adopted in preliminary slamming assessments and is representative of the bow flare area under head-sea conditions. At this point, both absolute and relative motions were computed for vertical displacement and pitch-induced rotation. For heave, the absolute vertical displacement is denoted by $s_3(t)$, and the wave elevation at the same location is $\zeta_P(t)$. The relative vertical displacement between the hull and the wave at point P is therefore expressed according to Equation (5):

$$r_3(t) = s_3(t) - \zeta_P(t) \quad (5)$$

Pitch-induced contributions to the vertical motion at this location were also taken into account, based on the pitch angle $\eta_5(t)$ and the longitudinal offset of point P from the CG. The resulting combined vertical response, which includes both heave and pitch effects, is given by Equation (6):

$$r(t) = \eta_3(t) - \zeta_P(t) + x_P\,\eta_5(t) \tag{6}$$

Where x_P is the longitudinal distance from the CG to point P, taken positive in the forward direction. The relative vertical velocity at this point is then obtained by differentiating Equation (6) with respect to time, as shown in Equation (7):

$$v(t) = r(t)\,\eta_3(t) - \zeta_P(t) + x_P\,\eta_5(t) \tag{7}$$

These quantities were computed in the frequency domain and stored in amplitude-phase format, such as r_A, ε_R for displacement and v_A, ε_V for velocity, to support later analyses of slamming occurrence and hydrodynamic performance comparison. To represent realistic sea conditions, irregular wave responses were evaluated using spectral analysis. The Bretschneider spectrum, defined by Equation (8), was adopted to describe the wave energy distribution:

$$S_\zeta = \frac{173 H_{1/3}^2}{T_1^4}\,\omega^{-5}\exp\left\{\frac{-692}{T_1^4}\,\omega^{-4}\right\} \tag{8}$$

Where $H_{1/3}$ is the significant wave height and T_1 is the mean wave period. The corresponding motion response spectrum for each motion component $\eta(\omega)$ was calculated using Equation (9):

$$S_\eta(\omega) = |\mathrm{RAO}_\omega|^2 * S_\zeta(\omega) \tag{9}$$

Finally, the zeroth-order spectral moment, used later in the slamming probability formulation, was obtained by numerical integration of the motion spectrum, as shown in Equation (10):

$$m_0 = \int_0^\infty S_\eta(\omega)d\omega \tag{10}$$

These spectral moments were evaluated for both relative displacement and velocity at point P. In combination with long-term sea statistics, they form the basis for the probabilistic assessment of slamming events. To ensure that the computed responses reflect realistic and demanding operational conditions, wave data were extracted from the Octopus statistical database for a region near the southern tip of South America, where adverse sea states are frequent. The joint probability distribution of significant wave height and mean wave period used in this study is shown in Figure 3. These values were applied to compute weighted slamming probabilities across multiple sea states, incorporating real-world operational variability into the evaluation.

3.3. Slamming Predictions

The probabilistic estimation of slamming occurrence in this study is based on the method originally proposed by

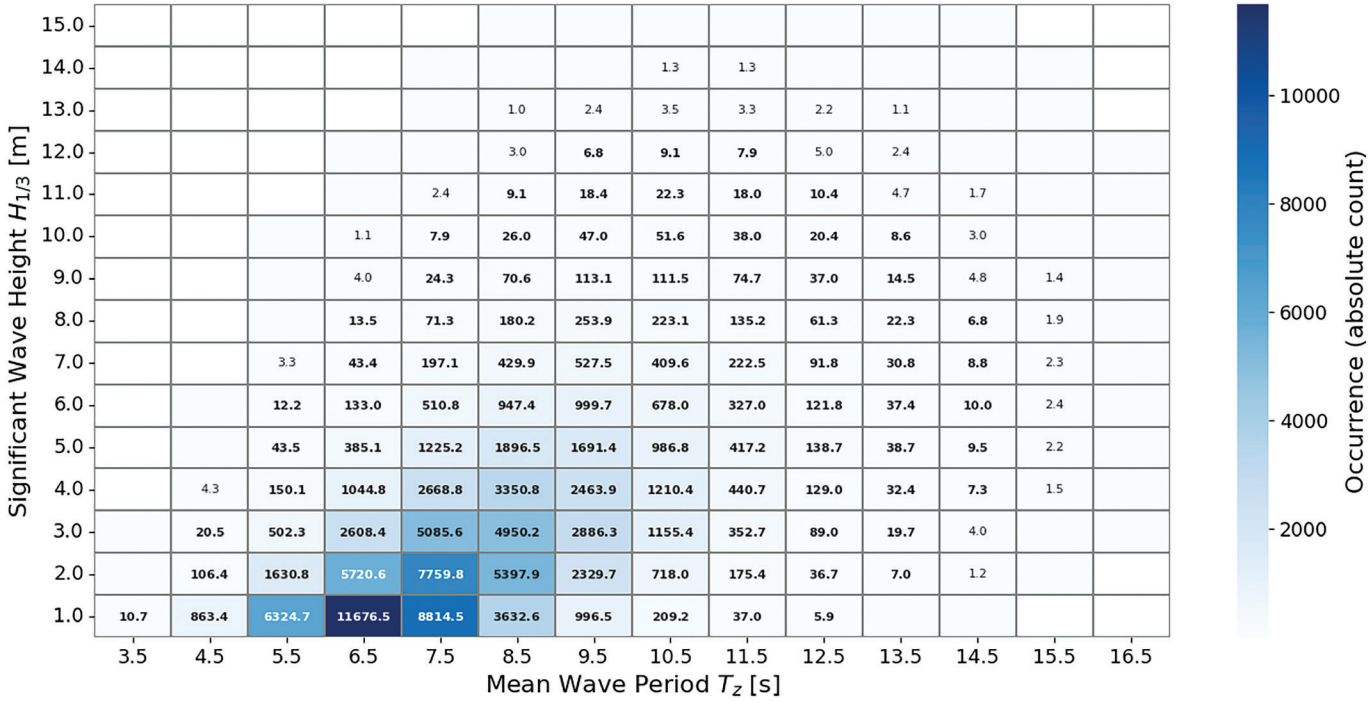

Figure 3. Joint probability distribution-South Atlantic Region.

Ochi [11], which defines the event as resulting from the simultaneous occurrence of two statistically independent conditions at a critical point on the hull: 1) emergence of the point above the free surface, and 2) its reentry with a vertical velocity exceeding a critical threshold. This dual-condition approach provides a simplified yet robust framework for evaluating slamming frequency in irregular seas. In this study, the critical point P is located at 10% of the ship's length from the bow along the keel, where slamming is most likely to occur. To model sea conditions, the Bretschneider spectrum was employed to represent irregular waves. For each sea state in the long-term database, the zeroth-order spectral moments of displacement and velocity at poin P — m_{OS} and m_{OV}, respectively—were computed. These values serve as the basis for evaluating the probability of each slamming condition. The critical reentry velocity V_{CR} was computed using the empirical expression derived by [12], based on Froude similarity [Equation (11)]:

$$V_{CR} = 0.093\sqrt{gL} \tag{11}$$

The probability that the vertical velocity v_3 at point P exceeds this critical threshold is given by Equation (12):

$$\Pr\{v_3 > V_{CR}\} = \exp\left(-\frac{V_{CR}^2}{2m_{OV}}\right) \tag{12}$$

Simultaneously, the probability that the absolute displacement at P exceeds the local draft T_P is defined by Equation (13):

$$\Pr\{s_3 > T_P\} = \exp\left(-\frac{T_P^2}{2m_{OS}}\right) \tag{13}$$

Assuming statistical independence between the two conditions, the overall probability of slamming per wave cycle is computed using Equation (14):

$$\Pr\{\text{Slam}\} = \exp\left(-\frac{T_P^2}{2m_{OS}} - \frac{V_{CR}^2}{2m_{OV}}\right) \tag{14}$$

To obtain long-term probability estimates, the results were weighted by the joint probability distribution of significant wave height and mean wave period, as shown in Figure 2. The weighted formulation is expressed in Equation (15):

$$\Pr(\text{Slam})_{\text{Total}} = \sum_{i=1}^{n}\Pr(\text{Slam})_i \Pr\left(H_{1/3}, T_Z\right)_i \tag{15}$$

The mean encounter period at point P, based on the spectral moments, is given by Equation (16):

$$T_{2S} = 2\pi\sqrt{\frac{m_{OS}}{m_{OV}}} \tag{16}$$

Thus, the expected number of slamming events per hour is computed according to Equation (17):

$$N_{\text{Slams/hr}} = \frac{3600}{T_{2S}}\Pr(\text{Slam})_{\text{Total}} \tag{17}$$

4. Results and Discussion

4.1. Hydrodynamic Coefficients

To assess the hydrodynamic effects of hull form variation, frequency-dependent coefficients were calculated for heave and pitch motions using linear strip theory. Among the four investigated parameters, the block coefficient (C_B) and the waterplane area coefficient (C_{WP}) produced the most expressive variations in excitation and radiation components.

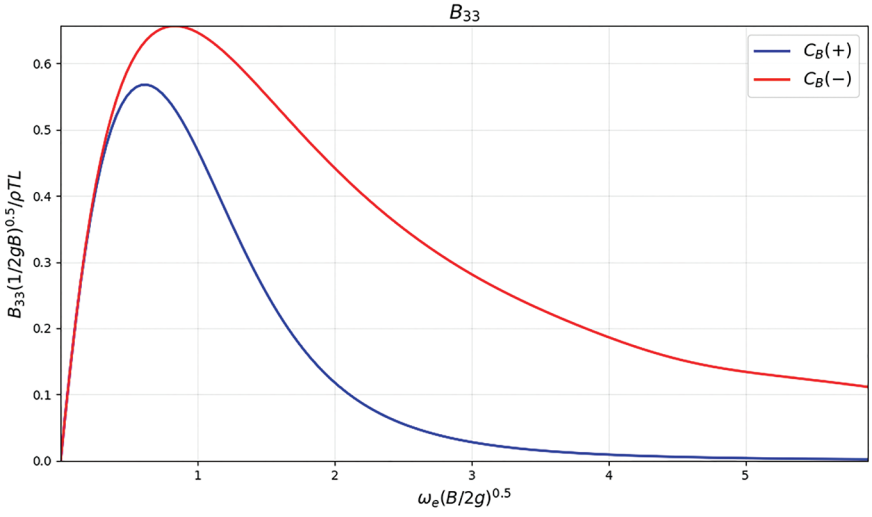

Figure 4. Damping coefficient B_{33} for C_B variants (adapted from [8]).

Therefore, only the most representative coefficients, specifically the heave damping coefficient B_{33} and the pitch restoring stiffness C_{55}, were selected for discussion. Other hydrodynamic terms, such as B_{55} or C_{33}, showed minimal variation across the hull variants and were omitted for brevity. Figure 4 presents the damping coefficient B_{33} for the C_B(+) and C_B(-) configurations. The finer hull form C_B(-) exhibits slightly higher damping values across most of the analyzed frequency range, particularly near the region of maximum response. This behavior aligns with expectations, as more slender geometries promote stronger wave radiation due to reduced sectional area and increased curvature near the bow and stern.

Figure 5 displays the hydrostatic restoring coefficient C_{55} for the C_{WP}(+) and C_{WP}(-s) models. Increasing the waterplane area coefficient significantly enhances the hydrostatic restoring moment in pitch, reinforcing the importance of waterplane geometry in seakeeping performance, especially regarding pitch stability. Other coefficients such as B_{55}, C_{33} and excitation terms F_3 and F_5 were also evaluated for C_{WP} variants but exhibited either low sensitivity or trends similar to those already presented. For brevity and focus, only the most relevant terms are included in this discussion.

4.2. Relative Motion and Velocity

Relative vertical displacements and velocities at the keel point P, located 10% of L_{PP} aft of the bow, were computed for all hull variants. As introduced in Section 4.2, the relative motion is defined as the difference between the vertical displacement of the hull and the local wave elevation at the same location [see Equation (5)]. This quantity is directly related to the occurrence of slamming events. In addition, the vertical relative velocity is essential for the probabilistic estimation of slamming, as it determines the kinetic severity of impact upon water reentry. Figures 6 through 9 present the relative displacement amplitude r_3 at point P for each pair of extreme hull variants, corresponding to variations in *LCB*, C_B, *LCF*, and C_{WP}. Each configuration shows distinct dynamic behavior, demonstrating how isolated geometric changes affect bow response. Figure 6 compares *LCB*(+) and *LCB*(-) variants.

Figure 7 presents C_B(+) and C_B(-). The fuller hull shape (C_B+) exhibits higher vertical motion amplitudes, especially near the peak response region. The lower damping and greater

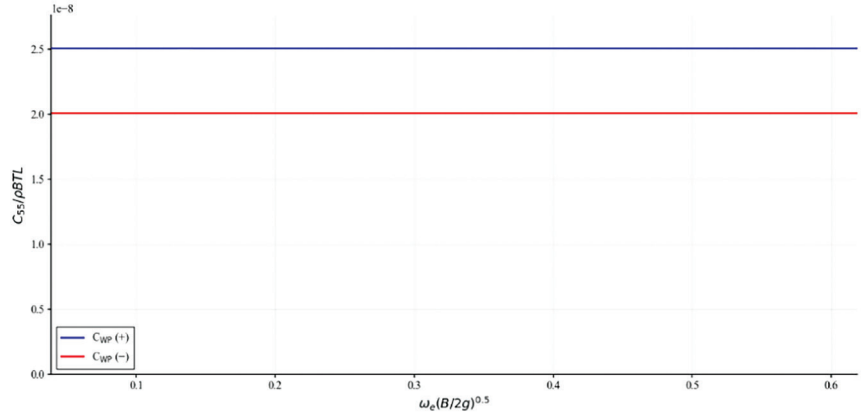

Figure 5. Restoring coefficient C_{55} for C_{WP} variants (adapted from [8]).

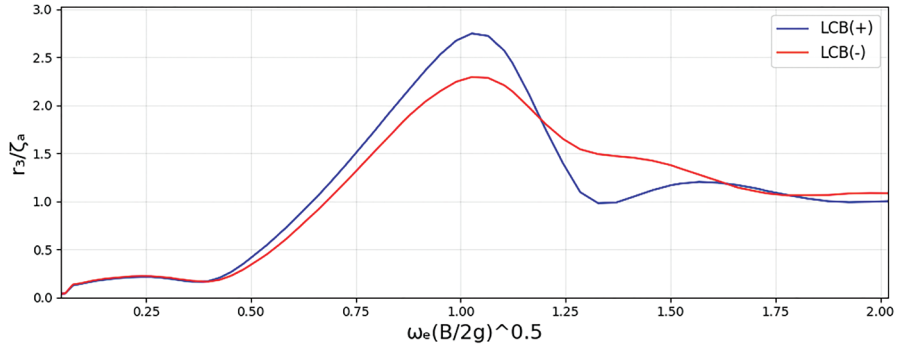

Figure 6. Relative vertical motion amplitude r_3 at point P for *LCB*(+) and *LCB*(-) configurations.

volume distribution in C_B(+) contribute to this amplification of bow dynamics.

Figure 8 shows results for *LCF*(+) and *LCF*(-). The *LCF*(-) variant, with its center of flotation positioned aft, demonstrates higher relative motion at point P, likely due to more pronounced pitch movement, which accentuates bow lift and drop.

Figure 9 highlights the impact of waterplane area. The C_{WP}(-) variant, representing a reduced waterplane, shows significantly increased motion amplitude. This configuration leads to lower hydrostatic stiffness and more abrupt responses to wave excitation.

Figure 10 summarizes the vertical relative velocity amplitude at point P for all geometric variants. As expected, the trends observed are closely aligned with those of the relative displacement: configurations that lead to higher vertical excursions [such as *LCB*(+), C_B(+), *LCF*(-), and C_{WP}(-)] also result in increased vertical velocities. These results reinforce the role of hull form in modulating the severity of water reentry and support the use of relative

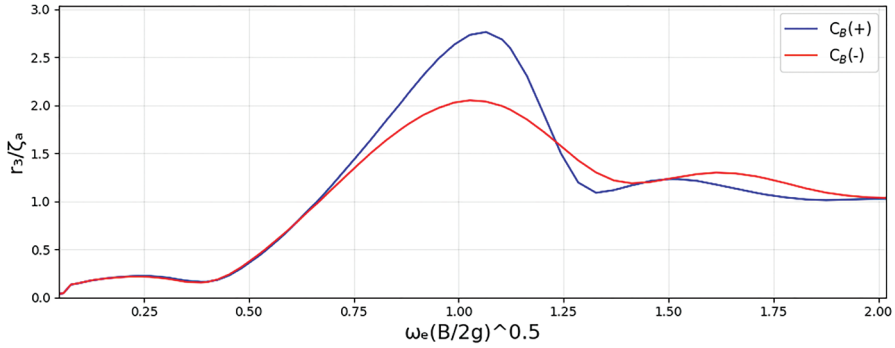

Figure 7. Relative vertical motion amplitude r_3 at point P for C_B(+) and C_B(-) configurations.

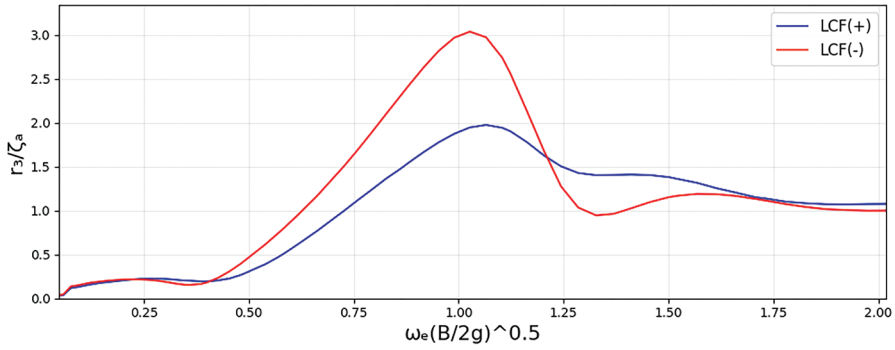

Figure 8. Relative vertical motion amplitude r_3 at point P for *LCF*(+) and *LCF*(-) configurations.

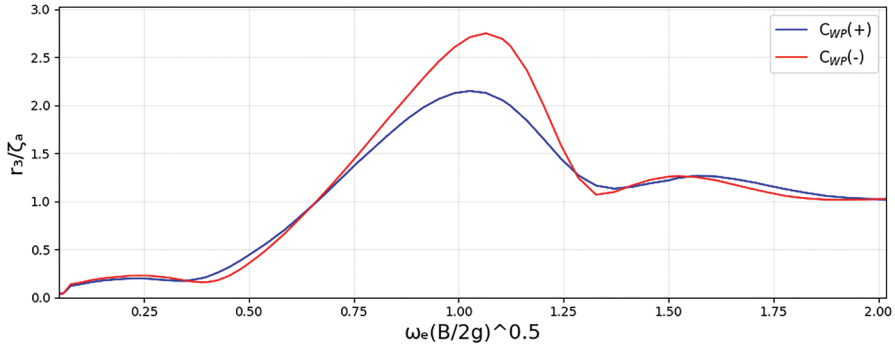

Figure 9. Relative vertical motion amplitude r_3 at point P for C_{WP}(+) and C_{WP}(-) configurations.

velocity as a key variable in slamming probability estimations.

4.3. Slamming Ocurrence

To assess how variations in hull form affect the ship's vulnerability to slamming, the predicted slamming probability (PR{slam}) was computed for each of the eight extreme configurations. These results were derived from the spectral moments associated with relative vertical velocity at point P and integrated with long-term wave statistics, as described in Section 4.3. Table 3 summarizes the predicted probability of slamming and the corresponding number of events per hour. Notably, most hull variants remained within the operational threshold defined by RINAMIL (2007), which recommends a maximum of 20 slamming events per hour for safe operation.

To better quantify the influence of each form parameter, a sensitivity index was defined as the change in PR{slam} divided by the corresponding geometric variation (in percentage points), normalized as ΔPR/ΔGeom×100. This index allows for a direct comparison of how responsive slamming behavior is to a given parameter variation. The results show that *LCF* exhibits the highest sensitivity (7.79), indicating that even moderate shifts in the longitudinal center of flotation can substantially affect slamming incidence. The C_{WP} and *LCB* also demonstrate moderate sensitivity, while C_B shows the lowest influence, despite its significant geometric variation. These findings are visually reinforced in Figure 11, which plots the geometric variation against the corresponding PR{slam}.

5. Limitations of the Adopted Methodology

This work is based on linear strip theory formulated within a frequency-domain seakeeping framework. This approach assumes linearized free-surface boundary conditions, small-amplitude wave excitation, and linear superposition of responses. Although widely adopted in preliminary ship design due to its robustness and computational efficiency, these assumptions limit the ability of the model to represent strongly non-linear hydrodynamic phenomena.

Slamming is a transient event involving rapid variations in wetted surface area, localized impact pressures, and non-linear fluid-structure interaction effects. Phenomena such as bow flare slamming, time-varying buoyancy, and possible air entrapment are not explicitly resolved within linear potential flow theory. Moreover, the frequency-domain formulation does not capture short-duration time-domain impact peaks that may occur in severe sea states.

In this study, slamming susceptibility was inferred from relative motion criteria combined with long-term probabilistic analysis, rather than through direct computation of impact pressures. The results should therefore be interpreted as indicators of comparative trends among hull configurations, rather than detailed predictions of local structural loads.

Non-linear time-domain solvers or high-fidelity CFD approaches may therefore produce different absolute magnitudes of motion amplitudes and impact-related metrics, particularly under steep or breaking wave conditions. Such non-linear effects could influence peak responses and local load estimates. However, for comparative parametric investigations within a consistent hull family, relative

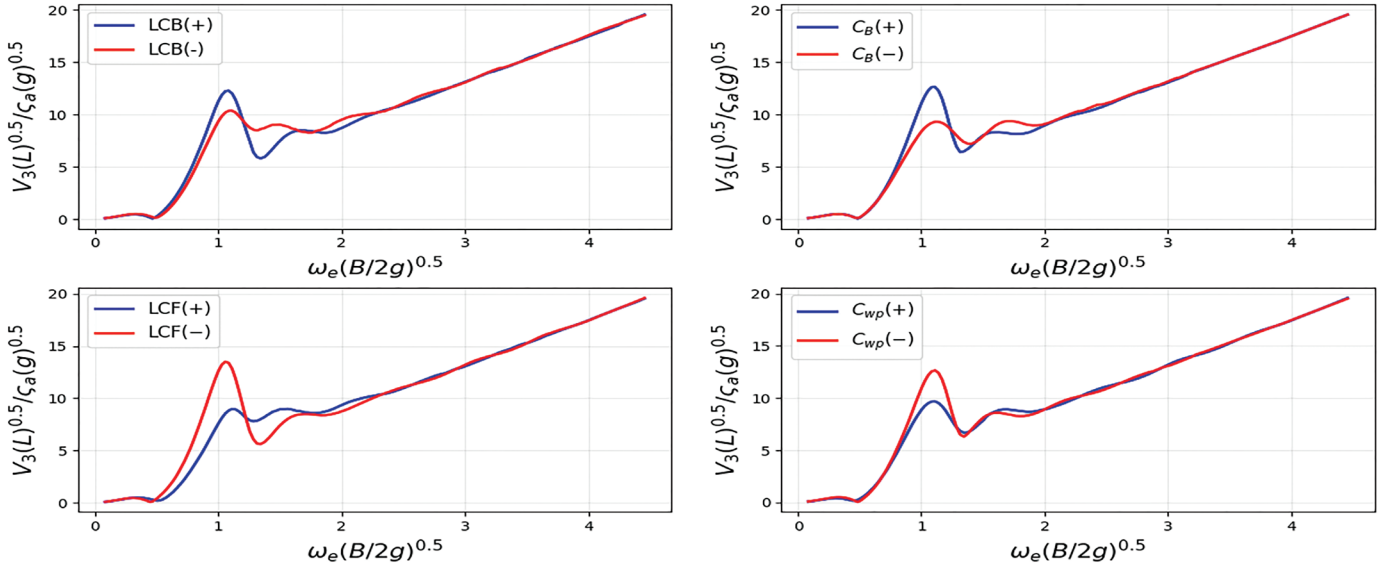

Figure 10. Relative vertical velocity amplitude at point P for all hull form variants.

sensitivity trends are expected to be less affected by these non-linear corrections.

The vessel was modeled as a rigid body, and hydroelastic effects were not considered. In addition, no dedicated experimental measurements or high-fidelity CFD simulations were performed for validation. While the adopted hydrodynamic framework is well established for preliminary seakeeping assessment, further validation through model testing or non-linear time-domain CFD analyses would improve the representation of impact phenomena.

The present analysis considered only heave and pitch motions, consistent with head-sea conditions. Surge, roll, and yaw were neglected under the assumption of symmetric wave encounter. However, in oblique or quartering seas, roll-pitch coupling and asymmetric bow immersion may influence slamming occurrence and severity. The inclusion of additional degrees of freedom in future time-domain analyses could provide a more comprehensive assessment of motion-impact interaction effects.

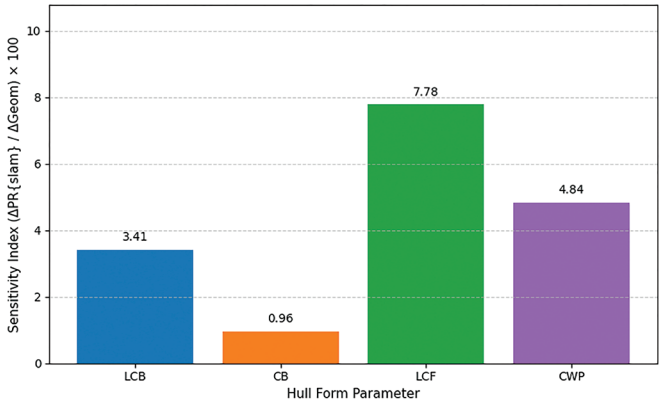

Figure 11. Sensitivity index (ΔPR{slam}/ΔGeom) for each hull form parameter.

The slamming assessment was restricted to a single longitudinal location (Point P at 10% L_{PP} from the forward perpendicular). Although this position is situated within the bow impact region typically adopted for preliminary slamming evaluations, slamming susceptibility may vary along the forward body depending on local flare geometry and entrance shape. A distributed longitudinal assessment considering multiple sections could reveal spatial sensitivity variations and further refine the interpretation of local impact risk.

Despite these limitations, the methodology remains suitable for comparative parametric studies aimed at identifying the relative sensitivity of hull form parameters to slamming susceptibility in early-stage design.

6. Conclusion

This study investigated the influence of key hull form parameters on the slamming susceptibility of a ship based on the hull geometry of the Friesland-class frigate, considering operation in a region near the southern tip of South America. This area is known for severe sea states, making it an ideal setting for evaluating slamming behavior under extreme wave conditions. By systematically varying *LCB*, C_B, *LCF*, and C_{WP}, eight extreme hull configurations were generated and analyzed. The assessment considered hydrodynamic coefficients, motion responses in waves, and a probabilistic evaluation of slamming based on long-term sea statistics.

Among the tested parameters, *LCF* and C_{WP}, which relate to the waterplane area, exhibited the strongest influence on slamming probability. An increase in these coefficients reduced the likelihood of bow immersion and thus slamming events. In contrast, volume-related parameters, particularly the block coefficient (C_B), had lower influence on the predicted slamming incidence. Notably, C_B exhibited the smallest variation in slamming probability, despite inducing the largest geometric modification among all parameters.

Table 3. Geometric variation, slamming probability, and sensitivity index for each hull form parameter.

Variant	PR{slam} (%)	Events/hour	ΔGeom (%)	ΔPR{slam} (%)	Sensitivity index (ΔPR/ΔGeom×100)
Baseline	1.03	19	-	-	-
LCB (+)	1.36	25	14.09	0.48	3.42
LCB (-)	0.88	17			
C_B (+)	1.33	25	64.80	0.62	0.96
C_B (-)	0.71	13			
LCF (+)	0.44	9	18.39	1.43	7.79
LCF (-)	1.87	34			
C_{WP} (+)	0.77	14	11.58	0.56	4.87
C_{WP} (-)	1.33	25			

This finding is particularly relevant for preliminary design. Since C_B greatly affects global ship geometry and displacement characteristics, its limited impact on slamming response suggests that it is the least suitable parameter to be used in optimizing hull form solely to mitigate slamming. From a design standpoint, the results support the use of targeted variations in *LCF* and C_{WP} as more effective and less intrusive strategies to control slamming. The introduction of a non-dimensional sensitivity index proved useful in quantifying how geometric changes translate into changes in slamming behavior, assisting early-stage design decisions.

As previously discussed, the adopted linear frequency-domain framework does not explicitly resolve non-linear impact phenomena. Nevertheless, for the purpose of comparative parametric assessment in the preliminary design stage, the methodology proved adequate in identifying relative slamming susceptibility trends among the investigated hull configurations. Further refinement through non-linear or high-fidelity approaches may enhance impact load prediction in future studies.

Footnotes

Financial Disclosure: The author declared that this study received no financial support.

NOMENCLATURE

$A(\omega)$	Added mass matrix
B	Beam at the waterline
$B(\omega)$	Radiation damping matrix
C_B	Block coefficient
C	Hydrostatic restoring matrix
CG	Center of Gravity
C_{WP}	Waterplane area coefficient
$F(\omega)$	Wave excitation force vector
$H_{1/3}$	Significant wave height
LCB	Longitudinal center of buoyancy
LCF	Longitudinal center of flotation
L_{PP}	Length between perpendiculars
S_η	Motion response spectrum
T	Draft
T_1	Mean wave period
T_{2S}	Mean encounter period
V_{CR}	Critical reentry velocity
m_0	Zeroth-order spectral moment
r	Relative displacement
s	Absolute displacement
v	Relative velocity
η	Motion response vector
ζ_a	Wave amplitude
ϕ	Velocity potential
ω	Encounter frequency

7. References

[1] G. K. Kapsenberg, “Finding the hull form for given seakeeping characteristics,” MARIN, Wageningen, the Netherlands, 2005.

[2] N. K. Bales, “Optimizing the seakeeping performance of destroyer type hulls,” in *Proceedings of the 13th ONR Symposium on Naval Hydrodynamics*, Tokyo, Japan, 1980.

[3] A. R. Lloyd, *Seakeeping: ship behaviour in rough weather*. Chichester, UK: Ellis Horwood Ltd., 1989.

[4] F. C. Belga, “Seakeeping optimization of a fast displacement catamaran on the basis of strip theory codes,” Master’s thesis, Instituto Superior Técnico, Lisbon, Portugal, 2017.

[5] M. L. Hakim, A. Firdaus, G. M. Ahadyanti, and T. Yulianto, “Comparative analysis of slamming phenomenon prediction between U and V hulls using strip theory method,” *Kapal: Jurnal Ilmu Pengetahuan dan Teknologi Kelautan,* vol. 19, no. 3, pp. 122-132, Oct 2022.

[6] X. Liao, Z. Chen, H. Gui, and M. Du, “CFD prediction of ship seakeeping and slamming behaviors of a trimaran in oblique regular waves,” *Journal of Marine Science and Engineering,* vol. 9, no. 10, p. 1151, Oct 2021.

[7] J. S. Gerritsma and W. E. Smith, “Full scale destroyer motion measurements,” *Journal of Ship Research,* vol. 11, no. 1, pp. 1-27, 1967.

[8] M. O. Predes, "Parametric analysis involving variations of form coefficients in slamming," Master's thesis, Federal University of Rio de Janeiro, Rio de Janeiro, Brazil, 2020. Available at: https://pantheon.ufrj.br/handle/11422/23176.

[9] M. O. Predes. "A simple combined method for parametric generation of ship hull variants," *Journal of Naval Architecture and Marine Technology*, vol. 227, pp. 52-63, 2025.

[10] N. T. Salvesen, E. O. Tuck, and O. M. Faltinsen, “Ship motions and sea loads,” *SNAME Transactions*, 1970.

[11] M. K. Ochi, “Prediction of occurrence and severity of ship slamming at sea”, in Proceedings of the 5th Symposium Naval Hydrodynamics, 1964.

[12] M. K. Ochi, and L. E. Motter, “A method to estimate slamming characteristics for ship design,” *Marine Technology,* vol. 8, 1971.